Editors' Suggestion

Metastable two-component solitons near an exceptional point

Dmitry A. Zezyulin [1,*] Yaroslav V. Kartashov [2] and Vladimir V. Konotop[3,†]
[1]*ITMO University, Saint Petersburg 197101, Russia*
[2]*Institute of Spectroscopy, Russian Academy of Sciences, Troitsk, Moscow 108840, Russia*
[3]*Departamento de Física and Centro de Física Teórica e Computacional, Faculdade de Ciências, Universidade de Lisboa, Edifício C8, Campo Grande, Lisboa 1749-016, Portugal*

(Received 28 April 2021; accepted 15 July 2021; published 4 August 2021)

We consider a two-dimensional nonlinear waveguide with distributed gain and losses. The optical potential describing the system consists of an unperturbed complex potential depending only on one transverse coordinate, i.e., corresponding to a planar waveguide, and a small nonseparable perturbation depending on both transverse coordinates. It is assumed that the spectrum of the unperturbed planar waveguide features an exceptional point (EP), while the perturbation drives the system into the unbroken phase. Slightly below the EP, the waveguide sustains two-component envelope solitons. We derive one-dimensional equations for the slowly varying envelopes of the components and show their stable propagation. When both traverse directions are taken into account within the framework of the original model, the obtained two-component bright solitons become metastable and persist over remarkably long propagation distances.

DOI: 10.1103/PhysRevA.104.023504

I. INTRODUCTION

Stable propagation of linear waves in either conservative or dissipative systems requires the reality of the spectrum of the governing evolution operator. When this operator is non-Hermitian and depends on control parameters, its spectrum can undergo qualitative changes upon variation of these parameters. In particular, the spectrum can change from purely real to a complex one. This (phase) transition between real and complex spectra typically occurs either through an exceptional point (EP) in the discrete spectrum [1–3] or through a spectral singularity in the continuous spectrum [4,5]. Although EPs as well as spectral singularities are introduced as characteristics of linear spectral problems [6], they also impact the propagation of nonlinear waves. First of all, stability of linear waves of a given nonlinear system is a necessary (although not yet sufficient) condition for stability of localized nonlinear waves, for example, of bright solitons (see Refs. [7,8] for review). An EP in the spectrum of the underlying linear system affects the equations governing weakly nonlinear waves having propagation constants in the vicinity of the EP [9,10]. If parameters of a nonlinear medium are close to an EP locally, i.e., only in a given spatial domain, a soliton interacting with such a domain can be scattered according to different scenarios [11]. In a waveguide geometry characterized by a separable optical potential (created by modulation of the dielectric permittivity) the existence of an EP in the linear spectrum of the carrying transverse modes of a separable optical potential can change the sign of the effective Kerr nonlinearity felt by a wave packet propagating along the waveguide [12].

In a more general context of nonlinear systems, an EP is sometimes introduced as a point of coalescence of the eigenvalues and eigenvectors of a *nonlinear* eigenvalue problem. The location of such an EP in the parameter space depends on the nonlinearity, i.e., on the amplitude of the field. This has been particularly well studied for models with double-well potentials [13–15], and it has also been found that the nonlinearity may have significant impact on the spectrum of the system in the vicinity of an EP. Thus, considering a nonlinear system with parameters at which its linear limit is close enough to an EP, one can expect fragility of the stability that may be destructively affected by the nonlinearity. Therefore, one may expect considerable constraints on stable propagation of nonlinear waves in such systems. In this paper, we show that this is not necessarily so: metastable solitons can exist even when the parameters of the underlying linear system are in close proximity to an EP.

The organization of our paper is as follows. In Sec. II we introduce a nonlinear planar waveguide, which is described by an optical potential depending on one of the transverse directions and features an EP. Then in Sec. III we develop a perturbation theory for the spectrum of the corresponding non-Hermitian evolution operator near the EP in the presence of a nonseparable perturbation depending on both transverse coordinates. In Sec. IV we derive the two-component system of equations governing evolution of the slowly varying amplitudes of the guided modes having the propagation constants in close proximity to the second-order EP. We employ the method of multiple-scale expansion where *two* coupled modes have to be accounted for for self-consistency of theory. The obtained system for slowly varying amplitudes features high-order dispersion, resembling (although not coinciding with) dispersion that may lead to pyramid diffraction, considered previously in Ref. [10]. In Sec. V we describe solitons of the derived effective one-dimensional (1D) model. Such solitons

*d.zezyulin@gmail.com
†vvkonotop@fc.ul.pt

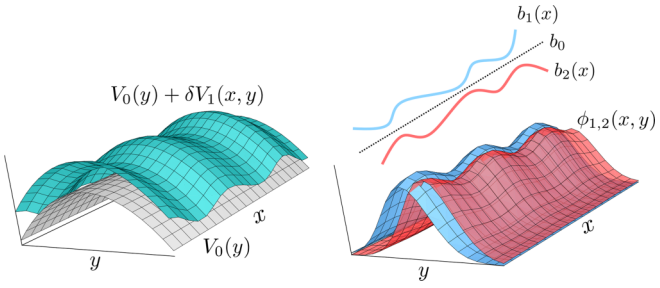

FIG. 1. Schematics of the geometry. The unperturbed potential $V_0(y)$ (left panel) features an EP at each value of x. For the perturbed potential $V_0(y)+\delta V_1(x,y)$ the degeneracy is lifted, and for each x the waveguide operates slightly below the EP, which means that for each x there are two close real-valued propagation constants, $b_1(x)$ and $b_2(x)$ (right panel), and two eigenfunctions $\phi_{1,2}(x,y)$ which are about to merge but nevertheless are distinct.

are stable in the 1D model and they become metastable in the full 2D model governing light propagation in the dissipative waveguide (Sec. VI).

II. THE MODEL

We consider propagation of a paraxial beam along the z direction in a medium with gain and losses modulated along the x and y directions. The amplitude of the field Ψ in dimensionless units is governed by the nonlinear Schrödinger equation

$$i\frac{\partial\Psi}{\partial z}=-\frac{1}{2}\nabla^2\Psi-V_\delta(x,y)\Psi+\chi|\Psi|^2\Psi, \tag{1}$$

where $\nabla=(\partial_x,\partial_y)$, the complex-valued optical potential $V_\delta(x,y)$ is parametrized by a real control parameter δ, and the real coefficient χ characterizes Kerr nonlinearity of the medium. Considering $0\leqslant\delta\ll 1$, we assume that the potential $V_\delta(x,y)$ can be represented in the form

$$V_\delta(x,y)=V_0(y)+\delta V_1(x,y). \tag{2}$$

Here $V_0(y)$ is a complex-valued potential for which the spectrum of the linear non-Hermitian Hamiltonian

$$H_0:=-\frac{1}{2}\partial_y^2-V_0(y) \tag{3}$$

has an EP $-b_0$ on the real axis, $b_0\in\mathbb{R}$, with $\phi_0(y)$ being the respective eigenfunction:

$$H_0\phi_0=-b_0\phi_0. \tag{4}$$

Schematics of the described waveguide are illustrated in Fig. 1. Since x does not enter Eq. (4), we can say that the waveguide has the EP at each value of x.

For further consideration, we define the associated (generalized) eigenfunction $\varphi_0(y)$,

$$(H_0+b_0)\varphi_0=\phi_0, \tag{5}$$

as well as the eigenfunction $\tilde\phi_0$ and the generalized eigenfunction $\tilde\varphi_0$ of the Hermitian conjugate $H_0^\dagger$:

$$H_0^\dagger\tilde\phi_0=-b_0\tilde\phi_0,\qquad (H_0^\dagger+b_0)\tilde\varphi_0=\tilde\phi_0. \tag{6}$$

Hereafter we use tildes for the spectral characteristics of the adjoint eigenvalue problem. In our case $H^\dagger=H^*$, and hence $\tilde\phi_0=\phi_0^*$ and $\tilde\varphi_0=\varphi_0^*$, where asterisks mean complex conjugation. We emphasize that neither ϕ_0 nor φ_0 depend on x; they depend only on y.

A signature of the EP is the orthogonality condition

$$\langle\tilde\phi_0,\phi_0\rangle=0. \tag{7}$$

Hereafter we use the inner product defined as

$$\langle f,g\rangle:=\int_{-\infty}^{\infty}f^*(x,y)g(x,y)dy. \tag{8}$$

Generally, the eigenfunction ϕ_0 is defined up to an arbitrary nonzero coefficient, and the generalized eigenfunction φ_0 is defined up to the addition of an arbitrary multiple of ϕ_0. It is convenient to fix these two functions by imposing the following normalization [16],

$$\langle\tilde\varphi_0,\phi_0\rangle=\langle\tilde\phi_0,\varphi_0\rangle=1, \tag{9}$$

and the orthogonality condition

$$\langle\tilde\varphi_0,\varphi_0\rangle=0. \tag{10}$$

III. PERTURBATION THEORY FOR THE SPECTRUM NEAR AN EP

Suppose, that $V_1(x,y)$ is chosen such that the spectrum of the perturbed linear Hamiltonian

$$H_\delta:=H_0-\delta V_1(x,y) \tag{11}$$

is all-real and there exist two eigenvalues, $b_1(x)$ and $b_2(x)$, i.e.,

$$H_\delta\phi_j(x,y)=-b_j(x)\phi_j(x,y),\quad j=1,2, \tag{12}$$

satisfying the condition

$$b_1(x)>b_0>b_2(x) \tag{13}$$

for all x. We recall that x plays the role of a parameter in the eigenvalue problem (12). We therefore can say that in the two-dimensional plane of parameters (δ,x) the Hamiltonian H_δ has an *exceptional line* $\delta=0$.

We also define the adjoint operator and eigenfunctions:

$$H_\delta^\dagger=-\frac{1}{2}\partial_y^2-[V_\delta(x,y)]^*=H_0^\dagger-\delta[V_1(x,y)]^* \tag{14}$$

and

$$H_\delta^\dagger\tilde\phi_j(x,y)=-b_j(x)\tilde\phi_j(x,y),\quad j=1,2. \tag{15}$$

Furthermore, we assume that H_δ does not have EPs when $\delta>0$ [this condition can be relaxed: what is really important for our consideration is the condition (13)]. Then the following biorthogonality relations hold:

$$\langle\tilde\phi_1,\phi_2\rangle=\langle\tilde\phi_2,\phi_1\rangle=0. \tag{16}$$

The structure of the eigenfunctions in the vicinity of the EP can be described in terms of the following asymptotic expansions ($j=1$ and 2):

$$\phi_j=\phi_0+(-1)^j\delta^{1/2}\rho_j+\delta\rho_{j1}+\delta^{3/2}\rho_{j2}+O(\delta^2), \tag{17a}$$

$$\tilde\phi_j=\tilde\phi_0+(-1)^j\delta^{1/2}\tilde\rho_j+\delta\tilde\rho_{j1}+\delta^{3/2}\tilde\rho_{j2}+O(\delta^2), \tag{17b}$$

at $\delta \to 0$. In Eqs. (17), the functions ρ_j and $\tilde{\rho}_j$ are so far undetermined corrections that generically depend on x and y. Since in the eigenvalue problem (12) x is a parameter, we can represent

$$b_j(x) = b_0 - (-1)^j \delta^{1/2} \beta_j(x) + \delta \beta_{j1}(x) + \delta^{3/2} \beta_{j2}(x) + O(\delta^2), \tag{18}$$

where the coefficients β_j, β_{j1}, and β_{j2} are to be found. Substituting Eqs. (17)–(18) in Eq. (12), one observes that the obtained equation in the leading order δ^0 is satisfied. The balance of the $\delta^{1/2}$-order terms requires that ($j = 1$ and 2)

$$(H_0 + b_0)\rho_j = \beta_j(x)\phi_0. \tag{19}$$

Comparing this equation with Eq. (5) we conclude that

$$\rho_j(x, y) = \beta_j(x)\varphi_0(y), \quad \tilde{\rho}_j(x, y) = \beta_j(x)\tilde{\varphi}_0(y). \tag{20}$$

Further, from the orthogonality condition (16) we obtain the relation $\delta^{1/2}(\beta_1 - \beta_2) + O(\delta) = 0$. Therefore

$$\beta_1(x) = \beta_2(x) =: \beta(x), \tag{21}$$

and hence

$$\rho_1(x, y) = \rho_2(x, y) = \beta(x)\varphi_0(y). \tag{22}$$

Now Eqs. (17a) and (17b) can be rewritten as

$$\phi_j = \phi_0 + (-1)^j \delta^{1/2} \beta(x)\varphi_0 + O(\delta), \tag{23a}$$

$$\tilde{\phi}_j = \tilde{\phi}_0 + (-1)^j \delta^{1/2} \beta(x)\tilde{\varphi}_0 + O(\delta), \tag{23b}$$

resulting in the normalization condition

$$\langle \tilde{\phi}_j, \phi_j \rangle = (-1)^j 2\delta^{1/2} \beta(x) + O(\delta). \tag{24}$$

To determine $\beta(x)$, we consider the next order, $O(\delta)$, of Eq. (12):

$$(H_0 + b_0)\rho_{j1} - V_1\phi_0 = \beta^2\varphi_0 - \beta_{j1}\phi_0. \tag{25}$$

Applying $\langle \tilde{\phi}_0, \cdot \rangle$, for either $j = 1$ or $j = 2$ we obtain

$$\beta^2(x) = -\langle \tilde{\phi}_0, V_1\phi_0 \rangle. \tag{26}$$

Obviously, our analysis is meaningful only if the right-hand side of Eq. (26) is positive. We also note that by choosing an appropriate $V_1(x, y)$, depending on both variables, x and y, one can obtain any desirable function $\beta(x)$, If, however, V_1 does not depend on y, then $\beta(x) = 0$. While Eq. (26) does not define the sign of β, the previously imposed convention (13) implies $\beta(x) > 0$ (notice that the inequality is strict).

Under the condition (26), a solution for Eq. (25) reads

$$\rho_{11} = f - \beta_{11}\varphi_0, \qquad \rho_{21} = f - \beta_{21}\varphi_0, \tag{27}$$

where f solves the equation

$$(H_0 + b_0)f = V_1\phi_0 + \beta^2\varphi_0. \tag{28}$$

The function f is defined up to the addition of an arbitrary multiple of ϕ_0, but from the following analysis it will become evident that without loss of generality this multiple can be set to zero.

Proceeding to the $O(\delta^{3/2})$ order, from Eq. (12) we obtain ($j = 1$ and 2)

$$(H_0 + b_0)\rho_{j2} = (-1)^j \beta(\rho_{j1} - \beta_{j1}\varphi_0 + V_1\varphi_0) - \beta_{j2}\phi_0. \tag{29}$$

Solvability conditions for these equations read

$$\beta_{j1} = \langle \tilde{\phi}_0, V_1\varphi_0 \rangle + \langle \tilde{\phi}_0, \rho_{j1} \rangle. \tag{30}$$

Substituting here ρ_{11} and ρ_{21} from Eq. (27), we obtain the next-order coefficients of the expansion for the propagation constants in the following form:

$$\beta_{11} = \beta_{21} = \tfrac{1}{2}\langle \tilde{\phi}_0, V_1\varphi_0 \rangle + \tfrac{1}{2}\langle \tilde{\phi}_0, f \rangle =: \gamma(x). \tag{31}$$

On the other hand, the orthogonality condition (16) in the $O(\delta)$ order requires

$$\gamma = \langle \tilde{\phi}_0, f \rangle. \tag{32}$$

Combining this expression with Eq. (31), we obtain

$$\gamma = \langle \tilde{\phi}_0, V_1\varphi_0 \rangle. \tag{33}$$

The requirement for the propagation constant to be real implies that the perturbation V_1 should be chosen to ensure the reality of the right-hand side of Eq. (33). If this condition is satisfied, then Eq. (33) and the relations

$$\langle \rho_{j1}, \tilde{\phi}_0 \rangle = \langle V_1\phi_0, \tilde{\varphi}_0 \rangle - \beta_{j1}, \tag{34}$$

obtained by applying $\langle \cdot, \tilde{\varphi}_0 \rangle$ to Eq. (25), yield

$$\langle \rho_{j1}, \tilde{\phi}_0 \rangle = \langle \partial_x \rho_{j1}, \tilde{\phi}_0 \rangle = \langle \partial_x^2 \rho_{j1}, \tilde{\phi}_0 \rangle = 0. \tag{35}$$

Therefore, the estimate (24) can be improved as follows:

$$\langle \tilde{\phi}_j, \phi_j \rangle = (-1)^j 2\delta^{1/2} \beta(x) + O(\delta^{3/2}). \tag{36}$$

Finally, with the same accuracy we compute the following useful relations:

$$\langle \tilde{\phi}_k, \partial_x \phi_j \rangle = (-1)^j \beta_x \delta^{1/2} + O(\delta^{3/2}), \tag{37}$$

$$\langle \tilde{\phi}_k, \partial_x^2 \phi_j \rangle = (-1)^j \beta_{xx} \delta^{1/2} + O(\delta^{3/2}). \tag{38}$$

IV. MULTIPLE-SCALE EXPANSION

Now we turn to the nonlinear model and, using the multiple-scale expansion, look for the solution of Eq. (1) in the form

$$\Psi = \delta^{1/2} e^{i b_0 z} [\phi_1(x, y)U_1(x, z) + \phi_2(x, y)U_2(x, z)] + O(\delta^{3/2}), \tag{39}$$

where $U_1(x, z)$ and $U_2(x, z)$ are the envelopes of the two modes that coalesce in the EP in the limit $\delta = 0$. Thus, the field we are looking for is a two-component field. We substitute Eq. (39) into the main equation (1) and apply $\langle \tilde{\phi}_1, \cdot \rangle$ and $\langle \tilde{\phi}_2, \cdot \rangle$ to the resulting expression. Using the results of Sec. III, we arrive at a system of two coupled equations that govern the dynamics of U_1 and U_2:

$$i\partial_z U_1 = \mathcal{H}_0 U_1 - \delta^{1/2}\beta U_1 + \frac{\beta_{xx}}{4\beta} U_2 - \frac{\beta_x}{2\beta}\partial_x U_1 + \frac{\beta_x}{2\beta}\partial_x U_2 - \delta^{1/2}\frac{\chi_0}{2\beta}(U_1 + U_2)^2(U_1^* + U_2^*), \tag{40}$$

$$i\partial_z U_2 = \mathcal{H}_0 U_2 + \delta^{1/2}\beta U_2 + \frac{\beta_{xx}}{4\beta} U_1 + \frac{\beta_x}{2\beta}\partial_x U_1 - \frac{\beta_x}{2\beta}\partial_x U_2 + \delta^{1/2}\frac{\chi_0}{2\beta}(U_1 + U_2)^2(U_1^* + U_2^*). \tag{41}$$

Here

$$\mathcal{H}_0 = -\frac{1}{2}\partial_x^2 - \frac{\beta_{xx}}{4\beta}, \tag{42}$$

the effective nonlinearity is determined as

$$\chi_0 = \chi\,\langle \phi_0^*, |\phi_0|^2\phi_0\rangle, \tag{43}$$

and all terms of the order of δ (and higher) are neglected. Upon derivation of the system (40)–(41) we used that ($i, j, k = 1$ and 2)

$$\langle \tilde{\phi}_i, |\phi_j|^2\phi_k\rangle = \langle \phi_0^*, |\phi_0|^2\phi_0\rangle + O(\delta^{1/2}),$$
$$\langle \tilde{\phi}_i, \phi_j^2\phi_k^*\rangle = \langle \phi_0^*, |\phi_0|^2\phi_0\rangle + O(\delta^{1/2}).$$

Generally speaking, the effective nonlinearity coefficient χ_0 obtained in Eq. (43) is complex valued. However, it is necessarily real if the unperturbed potential is $\mathcal{P}_y\mathcal{T}$ symmetric. Here, according to standard definitions, the operator $\mathcal{P}_y$ corresponds to the reversal of the y axis, and the operator $\mathcal{T}$ corresponds to the complex conjugation, and thus $[\mathcal{P}_y\mathcal{T}, H_0] = 0$, where the unperturbed operator H_0 is defined in Eq. (3). Indeed, the $\mathcal{P}_y\mathcal{T}$ symmetry implies that $\mathcal{P}_y\mathcal{T}\phi_0 = e^{i\theta}\phi_0$, where θ is a constant phase. From Eqs. (5) and (9) it follows that $e^{2i\theta} = 1$; i.e., possible values of θ are 0 and π. In either case $\mathcal{P}_y|\phi_0|^2 = |\phi_0|^2$, and one can verify that χ_0 is real:

$$\begin{aligned}\langle \phi_0^*, |\phi_0|^2\phi_0\rangle &= \mathcal{T}\langle \phi_0, |\phi_0|^2\mathcal{T}\phi_0\rangle \\ &= \langle e^{-i\theta}\mathcal{P}_y\mathcal{T}\phi_0, |\phi_0|^2 e^{i\theta}\mathcal{P}_y\phi_0\rangle^* \\ &= e^{-2i\theta}\langle \mathcal{T}\phi_0, |\phi_0|^2\phi_0\rangle^* = \langle \phi_0^*, |\phi_0|^2\phi_0\rangle^*.\end{aligned}$$

Importantly, the effective nonlinearities for different components of the field, described by Eqs. (40)–(41), have opposite signs. This effect resembles the finding reported in Ref. [12], where it has been shown that the presence of an EP in the spectrum of the underlying linear problem can change the sign of the effective nonlinearity.

Equations (40)–(41) acquire a more convenient form if one introduces new functions $U_\pm = U_2 \pm U_1$ which satisfy the following system:

$$i\partial_z U_+ = -\frac{1}{2}\partial_x^2 U_+ + \delta^{1/2}\beta U_-, \tag{44a}$$

$$i\partial_z U_- = \left(-\frac{1}{2}\partial_x^2 - \frac{\beta_{xx}}{2\beta}\right)U_- - \frac{\beta_x}{\beta}\partial_x U_- + \delta^{1/2}\beta U_+ + \delta^{1/2}\frac{\chi_0}{\beta}|U_+|^2 U_+. \tag{44b}$$

The equations obtained for the envelopes make explicit the scaling of the solutions as well as constraints that should be imposed on the $\beta(x)$ dependence. Indeed, from Eq. (44a) we conclude that the envelope is smooth, in the sense that it depends on the scaled variables $\delta^{1/2}z$ and $\delta^{1/4}x$. From Eq. (44b) it follows that the consistency of the multiple-scale expansion requires $|\beta_x/\beta| \lesssim \delta^{1/4}$ and $|\beta_{xx}/\beta| \lesssim \delta^{1/2}$.

V. 1D SOLITONS AT CONSTANT β

Let us now consider solitons of the 1D model (44) at a constant $\beta > 0$, when $\beta_x = \beta_{xx} = 0$. For stationary solutions, $U_\pm = u_\pm(x)e^{i\mu z}$, the system (44) reduces to

$$\mu u_+ = \frac{1}{2}\frac{d^2u_+}{dx^2} - \delta^{1/2}\beta u_-, \tag{45a}$$

$$\mu u_- = \frac{1}{2}\frac{d^2u_-}{dx^2} - \delta^{1/2}\beta u_+ - \delta^{1/2}\frac{\chi_0}{\beta}|u_+|^2 u_+. \tag{45b}$$

The spectrum of the linear ($\chi_0 = 0$) limit of this system ($U_\pm \propto e^{i\mu z + ikx}$) has two branches:

$$\mu_\pm = -\frac{k^2}{2} \pm \sqrt{\delta}\beta. \tag{46}$$

System (45) can be further reduced to a fourth-order nonlinear equation:

$$-\frac{1}{4}\frac{d^4u_+}{dx^4} + \mu\frac{d^2u_+}{dx^2} + (\delta\beta^2 - \mu^2)u_+ + \delta\chi_0|u_+|^2u_+ = 0. \tag{47}$$

Two comments are in order. First, one can see that in the vicinity of the EP the governing equation includes the fourth-order dispersion, which corroborates the previous results on linear diffraction [9,10]. Second, the models similar to model (47) can be encountered in fiber optics in description of evolution of pulses close to the zero-dispersion wavelength (see, e.g., Refs. [17,18]).

A. Two-component solitons

Equation (47), and hence system (45), allows for an exact solution. Indeed, for $\chi_0 > 0$ and the propagation constant

$$\mu = \frac{5}{3}\delta^{1/2}\beta > \mu_+ \tag{48}$$

belonging to the semi-infinite gap of linear spectrum, one obtains [17]

$$u_+(x) = \beta\sqrt{\frac{10}{3\chi_0}}\,\mathrm{sech}^2\xi, \tag{49a}$$

$$u_-(x) = -\beta\sqrt{\frac{10}{3\chi_0}}\,(\mathrm{sech}^2\xi + \mathrm{sech}^4\xi), \tag{49b}$$

where for compactness we have introduced

$$\xi = \sqrt{\frac{\beta}{3}}\delta^{1/4}x. \tag{50}$$

The exact soliton given by Eq. (49) belongs to a continuous family parametrized by the propagation constant μ. Examples of such families are shown in Fig. 2(a) in the form of dependencies $P_\pm(\mu)$, where $P_\pm$ are the powers carried by each of the two components:

$$P_\pm = \int_{-\infty}^{\infty}|u_\pm(x)|^2dx. \tag{51}$$

B. Linear stability of two-component solitons

Now we proceed to the linear-stability analysis of the found solitons in the framework of the two-component model

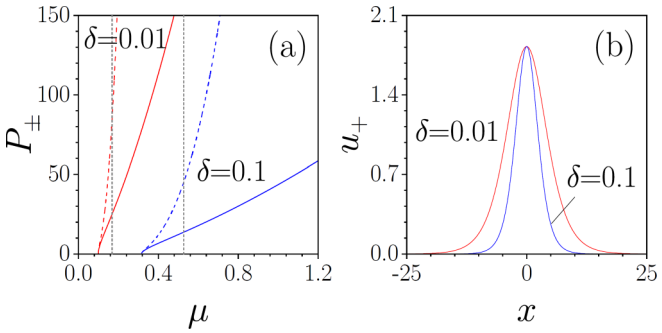

FIG. 2. (a) Families of solitons, in terms of the dependencies of powers $P_{\pm}$ on μ, for $\delta = 0.01$ (red curves) and $\delta = 0.1$ (blue curves). Solid and dashed lines correspond to P_+ and P_-, respectively. Gray vertical lines denote values of μ that correspond to the exact solution (48)–(49). (b) Profiles of corresponding exact solutions at $\mu = 0.167$ and $\delta = 0.01$ (red curve) and $\mu = 0.527$ and $\delta = 0.1$ (blue curve). Here $\chi_0 = 1$ and $\beta = 1$.

(44). For perturbed solutions in the form $U_{\pm} = e^{i\mu z}[u_{\pm}(x) + q_{\pm}(x, z)]$, where $q_{\pm}$ are small perturbations of real-valued solutions $u_{\pm}(x)$, the linearization of the two-component system (44) with constant β gives the following eigenvalue problem after splitting into real and imaginary parts:

$$\begin{aligned}
\partial_z \mathrm{Re}\, q_+ &= \mathcal{L}_0 \mathrm{Im}\, q_+ + \delta^{1/2}\beta \mathrm{Im}\, q_-, \\
\partial_z \mathrm{Im}\, q_+ &= -\mathcal{L}_0 \mathrm{Re}\, q_+ - \delta^{1/2}\beta \mathrm{Re}\, q_-, \\
\partial_z \mathrm{Re}\, q_- &= \mathcal{L}_0 \mathrm{Im}\, q_- + \delta^{1/2}(\beta + \chi_0\beta^{-1}u_+^2)\mathrm{Im}\, q_+, \\
\partial_z \mathrm{Im}\, q_- &= -\mathcal{L}_0 \mathrm{Re}\, q_- - \delta^{1/2}(\beta + 3\chi_0\beta^{-1}u_+^2)\mathrm{Re}\, q_+,
\end{aligned} \tag{52}$$

where $\mathcal{L}_0 = -(1/2)\partial_x^2 + \mu$. Making the substitution $(\mathrm{Re}\, q_+, \mathrm{Im}\, q_+, \mathrm{Re}\, q_-, \mathrm{Im}\, q_-) = e^{\omega z}(Q_+, R_+, Q_-, R_-)$, where ω is the linear stability eigenvalue (positive real part of ω corresponds to the exponential growth of the perturbation along the propagation distance), we then eliminate Q_- and R_- from the linear stability equations. This leads to athe *quadratic* eigenvalue problem

$$(\omega^2 \mathbb{1} + \omega\mathcal{C} + \mathcal{K})\mathbf{\Delta} = 0, \tag{53}$$

where

$$\mathbf{\Delta} = (Q_+, R_+)^T, \tag{54}$$

$$\mathcal{C} = \begin{pmatrix} 0 & -2\mu + \partial_x^2 \\ 2\mu - \partial_x^2 & 0 \end{pmatrix}, \quad \mathcal{K} = \begin{pmatrix} \mathcal{L}_+ & 0 \\ 0 & \mathcal{L}_- \end{pmatrix}, \tag{55}$$

$$\mathcal{L}_{\pm} = -\frac{1}{4}\partial_x^4 + \mu\partial_x^2 + (\beta^2\delta - \mu^2) + (2 \pm 1)\delta\chi_0 u_+^2, \tag{56}$$

and $\mathbb{1}$ is the identity operator. The quadratic eigenvalue problem (53) can be further converted into the generalized eigenvalue problem [19]

$$(\mathcal{A} - \omega\mathcal{B})\mathbf{Z} = 0, \tag{57}$$

where the augmented matrices read

$$\mathcal{A} = \begin{pmatrix} \mathcal{K} & 0 \\ 0 & -\mathbb{1} \end{pmatrix}, \quad \mathcal{B} = \begin{pmatrix} -\mathcal{C} & -\mathbb{1} \\ -\mathbb{1} & 0 \end{pmatrix}, \quad \mathbf{Z} = \begin{pmatrix} \mathbf{\Delta} \\ \omega\mathbf{\Delta} \end{pmatrix}.$$

Numerical solution of the generalized eigenvalue problem (57) indicates that the soliton families with $\chi_0 > 0$ are entirely stable.

C. Embedded soliton

For $\chi_0 < 0$, Eq. (47) admits another exact bright soliton solution which can be written down as [18]

$$u_+(x) = \beta\sqrt{\frac{10}{3|\chi_0|}}\,\mathrm{sech}\xi\,\tanh\xi, \tag{58a}$$

$$u_-(x) = \beta\sqrt{\frac{10}{3|\chi_0|}}\,\mathrm{sech}\xi\,\tanh^3\xi, \tag{58b}$$

where ξ is given by Eq. (50). The propagation constant of this solution,

$$\mu = -\frac{5}{6}\sqrt{\delta\beta^2}, \tag{59}$$

belongs to the continuous spectrum; i.e., this is an embedded soliton which can hardly be expected to be stable. The instability of this solution has indeed been confirmed by the linear-stability analysis (described in the previous section), as well as by using direct numerical simulations of one-dimensional propagation governed by the vector model (44). Nevertheless, the fact that the system derived here simultaneously supports bright solitons in both focusing and defocusing media is rather interesting.

VI. METASTABLE 2D SOLITONS

Now we turn to the two-dimensional solitons supported by the original model (1). To find stationary solutions, we use the substitution $\Psi(x, y, z) = e^{i\lambda z}w(x, y)$. Comparing this substitution with Eq. (39), we obtain the approximate relation $\lambda \approx b_0 + \mu$, which connects the propagation constant of the 2D solitons (i.e., λ) with that of the 1D solitons considered above in Sec. V. Using the exact solutions obtained above for the 1D model, one can produce a reasonable analytical approximation for the 2D soliton profile. At the same time, the feasibility of the experimental observation of such 2D solutions depends on the existence of the optical potentials $V_\delta(x, y)$ featuring an EP at $\delta = 0$ and purely real spectrum at $0 < \delta \ll 1$. Examples of such potentials are well known. We discuss two possible examples in the following subsections.

A. Exactly solvable $\mathcal{PT}$-symmetric Scarff II potential

Let $V_\delta(x, y)$ be the $\mathcal{P}_y\mathcal{T}$ Scarff potential [20–22]. For the analysis of its EP we use the representation (2) with

$$V_0 = \left[\frac{1}{4}(4\beta + 1)^2 - \frac{1}{8}\right]\mathrm{sech}^2 y + \frac{i}{4}(4\beta + 1)^2\mathrm{sech} y\tanh y, \tag{60}$$

$$V_1 = \frac{\mathrm{sech}^2 y}{2}. \tag{61}$$

For any positive $\beta > 0$, the potential $V_0(y)$ defined by Eq. (60) is exactly at the EP that corresponds to the coalescence of two eigenmodes at the propagation constant $b_0 = 2\beta^2$. The perturbation δV_1 increases the real part of the total potential

V_δ and therefore drives the system below the phase transition threshold.

Thanks to the solvability of the $\mathcal{PT}$-symmetric Scarf II potential [20–22], exact expressions for the propagation constants are available:

$$b_{1,2} = \frac{1}{8}[\sqrt{(4\beta+1)^2+\delta} \pm \sqrt{\delta} - 1]^2 = 2\beta^2 \pm \beta\sqrt{\delta} + \gamma\delta + O(\delta^{3/2}), \quad (62)$$

where [see Eqs. (31)–(33)]

$$\gamma = \frac{\beta}{2(4\beta+1)} + \frac{1}{8}. \quad (63)$$

The eigenfunctions at the EP read

$$\phi_0 = \frac{2^{2\beta+1} i\beta}{\sqrt{\pi}} \exp\left\{ i\frac{4\beta+1}{2} \operatorname{arctan\,sinh} y \right\} \operatorname{sech}^{2\beta} y, \quad (64)$$

$$\varphi_0 = \frac{\phi_0}{2\beta}[i \operatorname{arctan\,sinh} y - \ln \operatorname{sech} y - \psi(1) + \psi(4\beta) - \ln 2], \quad (65)$$

where $\psi(z) = d[\ln \Gamma(z)]/dz = \Gamma'(z)/\Gamma(z)$ is the digamma function [23]. One can check that the normalization conditions (9) are satisfied. The nonlinear coefficient defined by Eq. (43) is computed as

$$\chi_0 = -\chi \frac{16\beta^3}{3\pi \mathrm{B}(6\beta, 2\beta)}, \quad (66)$$

where $\mathrm{B}(\cdot,\cdot)$ is the beta function. Thus, $\chi_0 > 0$ ($\chi_0 < 0$) corresponds to the focusing (defocusing) nonlinearity of the physical model (1).

In Figs. 3(a) and 3(b) we compare analytical predictions for soliton shape (its cross section at $y = 0$) obtained using the combination of the exact 1D solution (49) and eigenfunctions given by Eqs. (64) and (65) with the numerically obtained 2D soliton of Eq. (1) having the same propagation constant $\lambda = 2\beta^2 + 5\delta^{1/2}\beta/3$. One can see that analytical and numerical solutions are very close at sufficiently small δ values, while with increases of δ the difference between them gradually increases.

B. Numerical results in the parabolic $\mathcal{PT}$-symmetric potential

For a more systematic study of the families of the 2D solitons, we choose a less sophisticated potential in the form

$$V_0 = -y^2 + i\gamma_0 y e^{-y^2/2}. \quad (67)$$

One-dimensional nonlinear modes in a potential of similar form have been considered in Ref. [24]. This potential has an EP at $\gamma_0 \approx 2.1684$. Analytical expressions for the eigenfunctions ϕ_0 and φ_0 are not available in this case, but they can be found numerically. In order to drive the potential V_0 to the unbroken $\mathcal{PT}$-symmetric phase, we perturb it by decreasing the gain-and-loss amplitude by means of the following perturbation:

$$V_1 = -i\frac{\beta^2}{0.5521} y e^{-y^2/2}. \quad (68)$$

Notice that the numerical coefficient in the denominator is chosen to ensure Eq. (26).

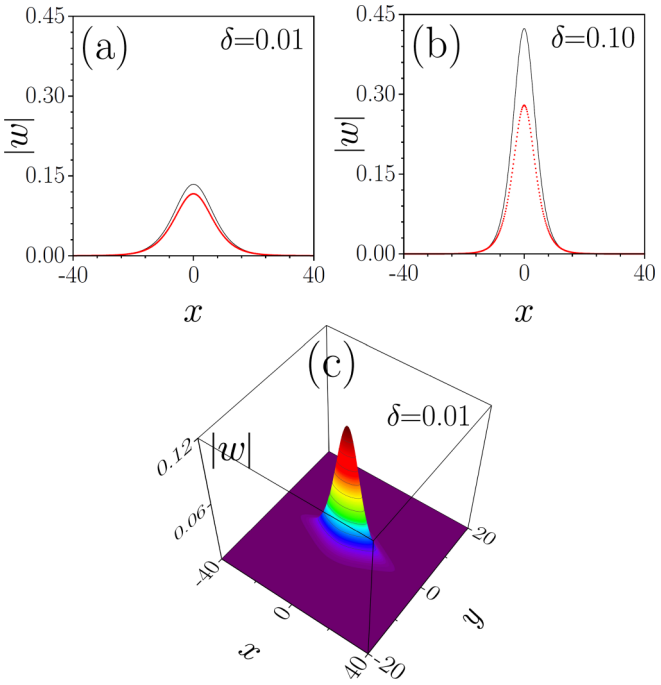

FIG. 3. (a, b) Comparison between analytical (black solid line) and numerical (red dots) soliton profiles in the $\mathcal{PT}$ Scarff potential for two values of δ. Here we show amplitudes of the solutions at fixed $y = 0$ as functions of x. (c) Three-dimensional plot of the numerical solution amplitude $|w(x, y)|$. In all panels $\beta = 0.4$ and $\chi = -1$.

A family of 2D solitons obtained numerically is shown in Fig. 4, where we present our results for the total power of solitons [cf. Eq. (51)],

$$P = \iint_{\mathbb{R}^2} |w(x,y)|^2 dx dy, \quad (69)$$

and for the soliton amplitudes and widths along the x and y axes. All these characteristics are functions of the propagation constant λ. While the analytical expression (39) is valid for soliton amplitudes $a \sim \delta^{1/2}$, the numerical continuation allows one to obtain even large-amplitude solitons. The cutoff value [shown with a dashed vertical line in Fig. 4(a)]

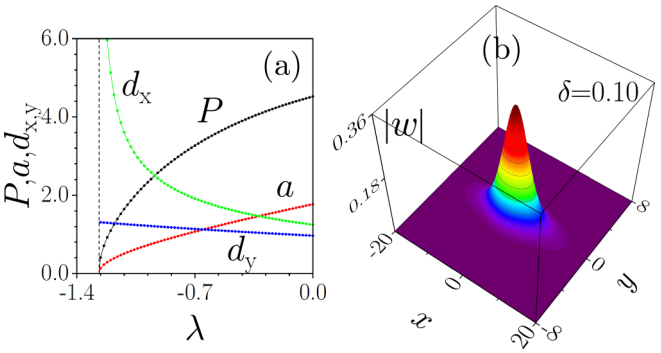

FIG. 4. (a) Dependencies of the power P, the peak amplitude a, and widths d_x and d_y on the propagation constant λ of 2D solitons in parabolic $\mathcal{PT}$-symmetric potentials at $\beta = 1$ and $\delta = 0.1$. (b) Profile of a stable soliton at $\lambda = -1.2$. The focusing nonlinearity coefficient $\chi = -1$.

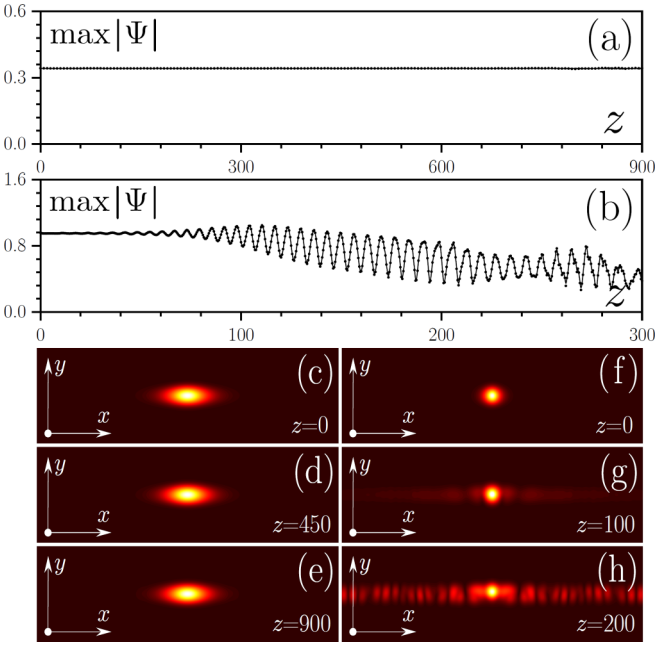

FIG. 5. Peak amplitude versus distance and field modulus distributions at different propagation distances for a stable 2D soliton with $\lambda = -1.2$ [panels (a) and (c)–(e)] and an unstable 2D soliton with $\lambda = -0.8$ [panels (b) and (f)–(h)] in a parabolic $\mathcal{PT}$ potential. In all cases $\beta = 1$ and $\delta = 0.1$. Panels (c)–(h) correspond to the spatial window $(x, y) \in [-40, 40] \times [-8, 8]$. The focusing nonlinearity coefficient $\chi = -1$.

corresponds to the edge of the continuum of two-dimensional scattering states. At the cutoff propagation constant, the soliton amplitude and power vanish. At the same time, the widths d_x and d_y illustrate the anisotropic nature of 2D solitons in our waveguide: as λ approaches the cutoff, the soliton width in the x direction diverges, while the width in the y direction remains finite.

While the stability analysis performed in Sec. V in the frame of the reduced 1D model for slowly varying envelopes has indicated that the 1D solitons are stable, this result does not yet guarantee stable propagation of the respective 2D solitons constructed using Eq. (39). A systematic numerical study of soliton propagation governed by the $(2 + 1)$D equation (1) indicates that near the cutoff value the 2D solitons are robust and propagate over considerable distances without noticeable distortions even in the presence of input perturbations, but far from the cutoff the oscillatory instabilities come into play, whose strength gradually increases with the increase of soliton amplitude and propagation constant. The example of metastable evolution of the 2D soliton is presented in Fig. 5(a), which shows that the amplitude of such a state remains practically unchanged with the distance z, while cross sections at different distances are shown in Figs. 5(c)–5(e). The example of instability development for a high-amplitude soliton stimulated by small input noise is presented in Figs. 5(b) and 5(f)–5(h). As one can see, such an unstable soliton starts radiating and at sufficiently large distance this radiation grows in amplitude and extends practically over the entire x cross section. We notice that weak oscillatory instabilities that affect propagation of the 2D solitons in our system can be possibly attributed to poorly localized (in the x direction) unstable modes that bifurcate from the interior of the two-dimensional continuum [25]. However, an accurate analysis of this issue requires a separate and more detailed study.

VII. CONCLUSION

In this work, we have shown that in a waveguide with gain and loss it is possible to obtain propagation of metastable two-dimensional solitons with propagation constants in the vicinity of the exceptional point (but belonging to the unbroken phase). Such solitons are effectively two-component solitons. Analytically they are described by the coupled linear and nonlinear Schrödinger equations which govern envelopes of the two carrier modes. The deviation of the propagation constant from the exceptional point is the small parameter of the multiple-scale expansion. The effective one-dimensional equations for the envelope allow for exact bright soliton solutions for either sign of the nonlinearity coefficient. The envelope solitons are stable in the one-dimensional setting, although they become metastable in the fully two-dimensional model. The lifetime of such solitons is very large, making them feasible for experimental observation.

ACKNOWLEDGMENTS

The work of D.A.Z. was supported by the Foundation for the Advancement of Theoretical Physics and Mathematics "BASIS" (Grant No. 19-1-3-41-1). V.V.K. acknowledges financial support from the Portuguese Foundation for Science and Technology (FCT) under Contract No. UIDB/00618/2020.

[1] C. M. Bender and S. Boettcher, Real Spectra in Non-Hermitian Hamiltonians Having $\mathcal{PT}$ Symmetry, Phys. Rev. Lett. **80**, 5243 (1998).

[2] C. M. Bender, Making sense of non-Hermitian Hamiltonians, Rep. Prog. Phys. **70**, 947 (2007).

[3] W. D. Heiss, The physics of exceptional points, J. Phys. A: Math. Theor. **45**, 444016 (2012).

[4] V. V. Konotop and D. A. Zezyulin, Phase transition through the splitting of self-dual spectral singularity in optical potentials, Opt. Lett. **42**, 5206 (2017).

[5] J. Yang, Classes of non-parity-time-symmetric optical potentials with exceptional-point-free phase transitions, Opt. Lett. **42**, 4067 (2017).

[6] T. Kato, *Perturbation Theory for Linear Operators* (Springer-Verlag, Berlin, 1980).

[7] V. V. Konotop, J. Yang, and D. A. Zezyulin, Nonlinear waves in $\mathcal{PT}$-symmetric systems, Rev. Mod. Phys. **88**, 035002 (2016).

[8] S. V. Suchkov, A. A. Sukhorukov, J. H. Huang, S. V. Dmitriev, C. Lee, and Y. S. Kivshar, Nonlinear switching and solitons in

$\mathcal{PT}$-symmetric photonic systems, Laser Photonics Rev. **10**, 177 (2016).

[9] S. Nixon, Y. Zhu, and J. Yang, Nonlinear dynamics of wave packets in parity-time-symmetric optical lattices near the phase transition point, Opt. Lett. **37**, 4874 (2012).

[10] S. Nixon and J. Yang, Pyramid diffraction in parity-time-symmetric optical lattices, Opt. Lett. **38**, 1933 (2013).

[11] Y. V. Bludov, C. Hang, G. Huang, and V. V. Konotop, $\mathcal{PT}$-symmetric coupler with a coupling defect: soliton interaction with exceptional point, Opt. Lett. **39**, 3382 (2014).

[12] B. Midya and V. V. Konotop, Waveguides with Absorbing Boundaries: Nonlinearity Controlled by an Exceptional Point and Solitons, Phys. Rev. Lett. **119**, 033905 (2017).

[13] H. Cartarius, D. Haag, D. Dast, and G. Wunner, Nonlinear Schrödinger equation for a $\mathcal{PT}$-symmetric delta-function double well, Phys. A: Math. Theor. **45**, 444008 (2012).

[14] A. S. Rodrigues, K. Li, V. Achilleos, P. G. Kevrekidis, D. J. Frantzeskakis, C. M. Bender, PT-symmetric double well potentials revisited: Bifurcations, stability and dynamics, Rom. Rep. Phys. **65**, 5 (2013).

[15] W. D. Heiss, H. Cartarius, G. Wunner, and J. Main, Spectral singularities in $\mathcal{PT}$-symmetric Bose-Einstein condensates, J. Phys. A: Math. Theor. **46**, 275307 (2013).

[16] A. A. Mailybaev, O. N. Kirillov, and A. P. Seyranian, Geometric phase around exceptional points, Phys. Rev. A **72**, 014104 (2005).

[17] N. N. Akhmediev and A. Ankiewicz, *Solitons: Nonlinear Pulses and Beams* (Chapman & Hall, London, 1997).

[18] A. Höök and M. Karlsson, Ultrashort solitons at the minimum-dispersion wavelength: effects of fourth-order dispersion, Opt. Lett. **18**, 1388 (1993).

[19] F. Tisseur and K. Meerbergen, The quadratic eigenvalue problem, SIAM Rev. **43**, 235 (2001).

[20] B. Bagchi and R. Roychoudhury, A new PT-symmetric complex Hamiltonian with a real spectrum, J. Phys. A: Math. Gen. **33**, L1 (2000).

[21] Z. Ahmed, Real and complex discrete eigenvalues in an exactly solvable one-dimensional complex $\mathcal{PT}$-invariant potential, Phys. Lett. A **282**, 343 (2001).

[22] G. Lévai, F. Cannata, and A. Ventura, Algebraic and scattering aspects of a $\mathcal{PT}$-symmetric solvable potential, J. Phys. A: Math. Gen. **34**, 839 (2001).

[23] *NIST Handbook of Mathematical Functions*, edited by F. W. J. Olver, D. W. Lozier, R. F. Boisvert, and C. W. Clark (Cambridge University, Cambridge, England, 2010).

[24] V. Achilleos Kevrekidis, D. J. Frantzeskakis, and R. Carretero-González, Dark solitons and vortices in $\mathcal{PT}$-symmetric nonlinear media: From spontaneous symmetry breaking to nonlinear $\mathcal{PT}$ phase transitions, Phys. Rev. A **86**, 013808 (2012).

[25] D. I. Borisov, D. A. Zezyulin, and M. Znojil, Bifurcations of thresholds in essential spectra of elliptic operators under localized non-Hermitian perturbations, Stud. Appl. Math. **146**, 834 (2021).